Radio Observations of IRAS 18043-2116:

A Post-AGB Water Maser Source

Fonda Day and Travis McIntyre

May 2007

Abstract

We present observations of water maser source IRAS 18043-2116 from February 18th, 2007. Observations were made in the radio at the 22GHz H_2O maser line with a velocity coverage of – 90 km/s to +200 km/s, using the Very Large Array (VLA) in D configuration. We discuss comparisons with previous observations of the same source and present a previously unobserved velocity range of the source spectrum (- 90 km/s < v < - 20 km/s).

I. Introduction

1.1. Masers

Microwave amplification by stimulated emission of radiation (maser) is a process in astronomy that exponentially increases source intensity. If there is a radiation source behind a gas (i.e. circumstellar envelope) that has undergone population inversion, then the source radiation can be amplified by traveling through the gas. A population inversion in a gas occurs when an energy pump continually excites the gas's electrons to a level where they are in a quasi-stable state such that more of the particles are in an excited state than are not. A photon with the same energy as the excited state, moving in the same direction (called velocity coherence) can de-excite the electron so that it produces another photon (illustrated in **Figure** 1) with the same frequency, phase, and direction of propagation. Now there are two photons where once there was one. These two travel on to make four, which produce eight, and so on. This is how a maser works. The gain received by a maser depends on the velocity coherence along the line of sight and exponentially on the thickness of the gas.

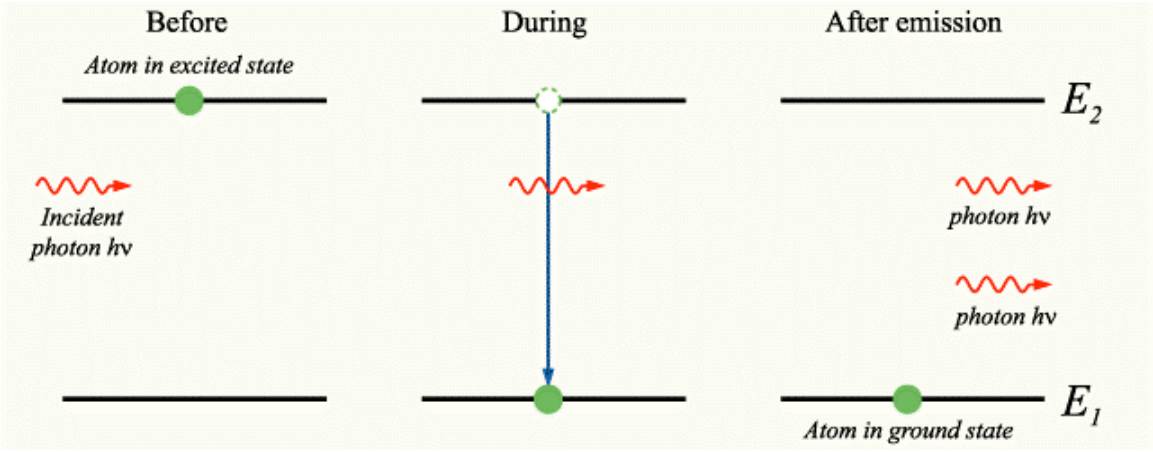

Figure 1. Illustration of stimulated emission by a maser and resulting amplification of source intensity. In this figure, $E_2 - E_1$ must equal hν. *Image derived from Image:Stimulatedemission.png

1.2. Post AGB Stars

A mid-sized star (<8$M_{\odot}$) like our Sun expands and becomes a red giant as it stops burning hydrogen into helium in the core and starts fusing it in shells around the star's nucleus. Luminosity increases sharply as this causes the atmosphere to expand, but the star cannot fuse the helium core without higher temperatures. Eventual core contraction allows core fusion of helium to begin and luminosity drops as the star once again becomes stable. Once all the core helium has been completely fused to carbon and oxygen, outer shells of hydrogen (and sometimes helium) begin fusing and the star expands again. The star is now on the asymptotic giant branch (AGB), because it approaches the increase in luminosity rate that was seen when the star was a red giant (illustrated in **Figure 2**). Next, the star will become a planetary nebula (PN) by ejecting most of its mass at once while the core shrinks to become a white dwarf. In between these two stages, called the post-AGB or proto-planetary nebula stage, stellar winds and violent pulsations cause the star to lose a lot of mass. This can allow for a collision population inversion in a surrounding circumstellar envelope, meaning it can create a maser gas. Subsequently, radiation from the post-AGB star is amplified by traveling through this maser, allowing us to detect it.

Studying post-AGB stars may help discern the processes behind part of stellar evolution. PN vary widely in shape, symmetry, and structure. They can be spherical, elliptical, bimodal, or irregular and the specific reasons for this are as of yet unclear. Studying the phase just before a star becomes a planetary nebula may give insight into the nature of PN formation — when and why asymmetries first form.

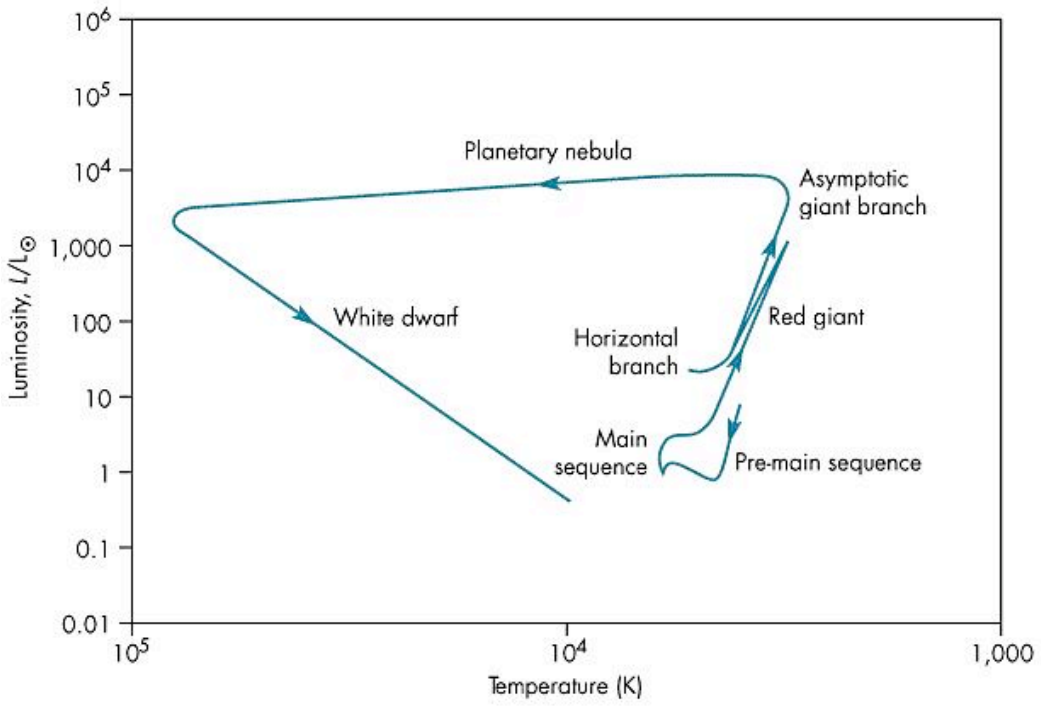

Figure 2. A stellar evolutionary track in the HR diagram with the main stages labeled. *Image taken from iapetus.phy.umist.ac.uk

1.3. IRAS 18043-2116

IRAS 18043-2116 (IRAS, b292, OH 0.9-0.4) is an infrared source believed to be a young post-AGB star. Both OH (1612 MHz, 1665 MHz, and 1720 MHz) and H_2O (22 GHz) maser emission has been detected from IRAS (Deacon et al. 2004, Sevenster & Chapman 2001, Deacon et al. 2007). Sevenster & Chapman (2001) do not detect continuum emission at 4.8 and 8.6 GHz, making it unlikely that IRAS 18043-2116 corresponds with a star forming region because these contain compact HII clouds that would produce continuum emission. It is also unlikely that this source is produced by a supernova remnant, because the 1720 MHz emission line has never been seen in supernova remnants. Hence, Sevenster & Chapman (2001) proposed that it is a post-

AGB star and that the 1720 MHz line was caused by a C-type shock, where densities would be high enough to produce H_2O molecules just behind the shock front, and that the dissociation of these H_2O molecules is what would produce the OH 1720 MHz emission. It was not expected, however, that densities would be high enough for the H_2O emission to be seen itself. With the observations of H_2O emission by Deacon et al. (2007), it is now believed that high-velocity jets of post-AGB stars are dense enough for this type of emission.

In the following sections, the observations, data reduction, and results of our study of H_2O emission from IRAS 18043-2116 are presented. Also, we compare our February 2007 results with earlier results from Deacon et al. (2004, 2007).

II. Observations and Data Reduction

We made spectral line observations of H_2O 22.235080 GHz maser emission from IRAS 18043-2116 on 18 February 2007 with the Very Large Array (VLA) in its D configuration. J1833-210 was used for phase calibration (~6.5° away), with a 1.3 minute switching cycle, and the flux calibrator was J0137+331. We used two frequency setups, to give a total velocity coverage of -93 km/s—203 km/s (total bandwidth of 6 MHz with 32 channels), with 3 km/s resolution. The first frequency setup covered -93 km/s—59 km/s, and the second setup covered 51 km/s—203 km/s. The resolution of the VLA in D configuration at 22 GHz is ~2.7 arcsec.

Eleven of the twenty seven antennas needed to be flagged in both frequency setups for the entire observing time because they either did not collect data (three of them) because of antenna shadowing, or were EVLA antennas (eight of them) that did

not collect data because of a script error. Furthermore, the second frequency setup had an additional antenna that did not collect data. **Table 1** lists the total on-source time, the number of useable antennas, and the expected thermal noise per channel for each frequency setup.

Table 1: Observation Parameters

	Time On-souce [s]	# Antennas	Expected Thermal Noise [mJy]
Frequency Setup 1	**580**	**16**	**2.9**
Frequency Setup 2	**420**	**15**	**3.6**

The sky was overcast during the observations, and the source was low in the sky (~ 20˚ attitudinally from horizon). We reduced the data using the *Astronomical Imaging Processing System* (*AIPS*). We flux- and phase-calibrated the data, as well as bandpass-corrected. The data was then self-calibrated and imaged using the *AIPS* task IMAGR. Self calibration was quite helpful, improving rms noise from ~ 30mJy to ~ 8mJy. The sources were unresolved within the beam, so a box was fit around the source and the *AIPS* task ISPEC was used to plot the intensity as a function of velocity, giving a water maser spectrum for the object. To reduce source "ringing" in the spectra, they were Hanning smoothed (as can be seen in **Figure** 3) and then averaged over two channels, which reduced the velocity resolution to ~ 6 km/s**.** Each maser peak was fitted to a single-component Gaussian to determine its integrated flux. For peaks whose emission appeared to span more than one channel, each channel's integrated flux was found, and then added together to give the total integrated flux of the maser peak (errors were added in quadrature to give the total error).

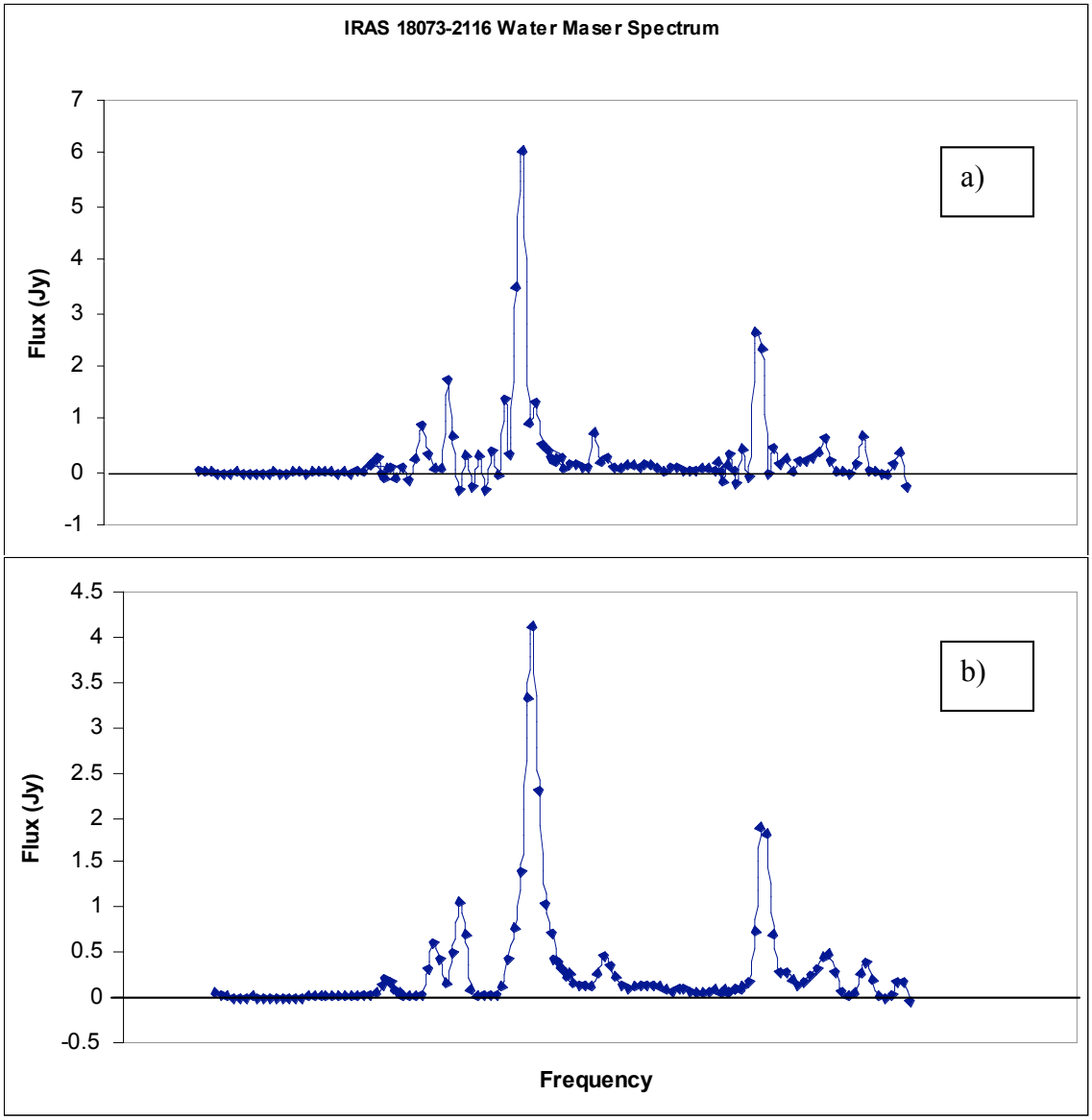

Figure 3. Comparison of a) "raw" spectrum, versus b) Hanning smoothed spectrum in arbitrary frequencies.

III. Results

H_2O emission was detected at RA 18:07:20.83 and DEC -21:16:13.4, in agreement with previously observed positions (Deacon, Chapman & Green 2004, Deacon et al 2007). We found multiple redshifted and blueshifted H_2O maser components in

IRAS 18073-2116. Eight components, of at least 30σ, and their fluxes are listed in **Table 2**, which can be seen in the complete spectrum from our observations listed below in **Figure 4**. All the data presented at v < -20 km/s is at a previously unobserved velocity coverage. The rms level reached in each IF was ~ 8 mJy, close to the expected thermal noise levels (see **Table 1**).

Table 2. Velocity and Fluxes of Each Maser Component

Velocity [*km/s*]	Integrated Flux [*Jy km/s*]	Peak Flux [*Jy*]
-74	0.356 +/- 0.008	0.356
-58	0.436 +/- 0.008	0.436
-32	2.02 +/- 0.01	2.02
35	0.562 +/- 0.008	0.39
65	7.25 +/- 0.02	3.3
96	0.092 +/- 0.008	0.092
107	0.548 +/- 0.008	0.548
128	0.26 +/-0.01	0.15

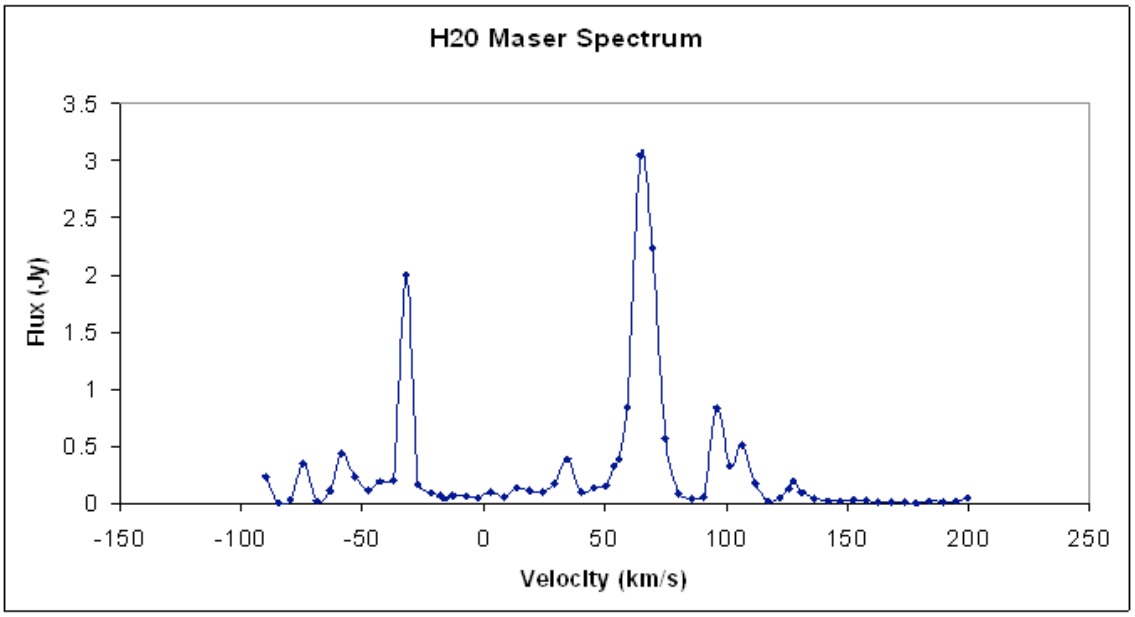

Figure 4. Smooth and averaged spectrum of IRAS 18043-2116 made from our observations in February 2007. Spectrum is graphed by calibrated flux versus Doppler shift from H_2O rest frequency in km/s.

IV. Discussion

The strongest peak from our data is at 70 km/s and has a peak flux of 3.3 Jy. Observations by Deacon et al. (2007) from 2004, with the Tidbinbilla telescope in Australia show only several minor components of < 1 Jy at 70 km/s. This same component was barely visible at 0.2 Jy in the 2002 data taken by Deacon, Chapman & Green (2004). Our results confirm that the maser spot at 70 km/s is real, and that it is variable and probably an unresolved combination of several spots. **Figure 5** shows our 2007 spectrum (top) compared to the Deacon et al. (2007) spectrum (bottom).

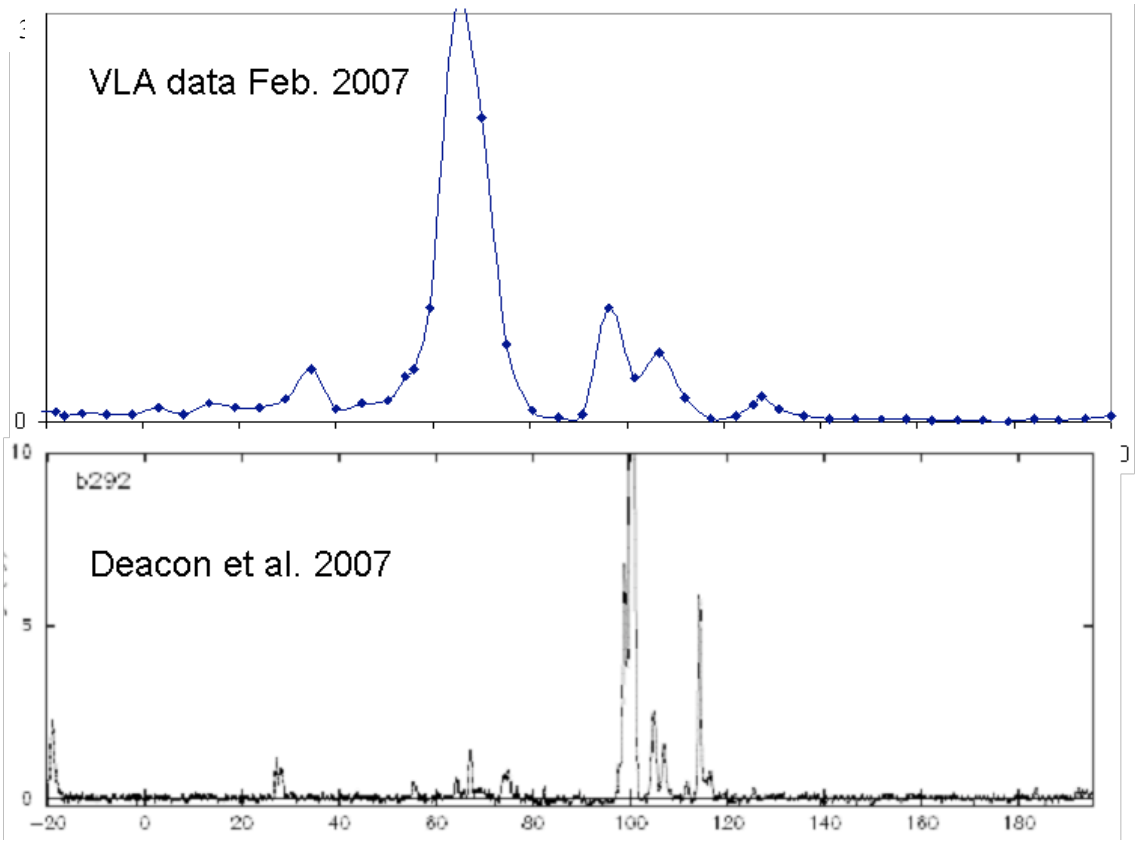

Figure 5. Comparison of our spectrum (top) from 2007 versus Deacon et al (2007) spectrum (bottom) from 2004, taken over the same velocity coverage. The flux scales are different for aesthetic purposes, however. Notice that the top spectrum only goes up to 3 Jy while the other goes up to 10 Jy.

There are clear maser spots in both our spectra in the range 100 km/s to 120 km/s, but with much variability. Deacon et al. (2007) detected a 25 Jy spot at 100 km/s which lessened to only a ~ 1 Jy peak in our data, and also two distinct ~ 2 Jy peaks at 106 km/s which were resolved out into one 0.5 Jy peak in our spectrum. Furthermore, Deacon et al. (2007) observed a ~ 0.5 Jy peak at 25 km/s which we might be seeing at 35 km/s. Much of our misalignments with the Deacon et al (2007) spectrum may be attributed to our lower velocity resolution, but comparisons can still be made and there is much variability between then and now. This suggests that either the pumping mechanisms for the different maser components are different or varying, or that the masers are in different spatial positions. We were unable to resolve the masers, so their positions relative to each other remain unknown.

It may be worthwhile to mention the peaks in the Deacon et al (2004) data taken in 2002 and presented in **Figure 6**. The peak at 106 km/s corresponds with both spectra above, as does arguably the spot at ~ 70 km/s. The spot at 85 km/s however, is completely absent in both previous mentioned observations. The spectrum from Deacon et al. (2004) does not show detectable emission at 100 km/s, which was seen two years later at 25 Jy (Deacon et al. 2007), and as a partially blended component in our data.

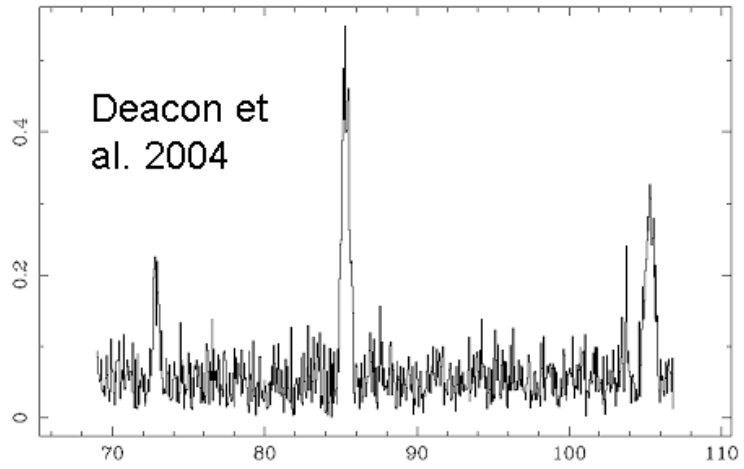

Figure 6. Deacon et al (2004) spectrum of IRAS from 2002 observations.

V. Conclusions

We have obtained the largest velocity coverage (-93 km/s—203 km/s) of 22 GHz H_2O maser emission from IRAS 18073-2116 up to date. At least eight components were visible in the spectra, though it is probable that many contain more than one "true" spot, and have resolved them out into one peak. Continued radio observations of IRAS 18073-2116 may give us a better understanding of the mechanisms behind the formation and subsequent structure of planetary nebula. This highly variable source is evidence that a post-AGB star in a surrounding that gives off maser emission is rich in complexities. Water maser observations of IRAS 18073-2116 should especially continue at the $v < -20$ km/s range, as we have detected three clear maser spots there and it would be advantageous to track their progress, including possibly detecting more components beyond -90 km/s. High resolution observations using VLBI may even resolve the maser components, which could shed new light on why some of the features are highly variable (e.g. the features around 100 km/s) while others are not.

References:

Deacon, R. M., Chapman, J. M., & Green, A. J. 2004, ApJS, 155, 595

Deacon, R. M., Chapman, J. M., Green, A. J. & Sevenster, M. N. 2007, ApJ, 658,1096

Killeen, N. E. B. 2001, A&A, 366, 481

Sevenster, M. N., van Langevelde, H. J., Moody, R. A., Chapman, J. M., Habing, H. J. &